JPP Journal of Pharmacy and Pharmacology

JPP 2008, 60: 977–985

Received October 29, 2007
Accepted March 20, 2008
DOI 10.1211/jpp.60.8.0005
ISSN 0022-3573

Radiotherapy enhancement with gold nanoparticles

James F. Hainfeld, F. Avraham Dilmanian, Daniel N. Slatkin and Henry M. Smilowitz

Abstract

Gold is an excellent absorber of X-rays. If tumours could be loaded with gold, this would lead to a higher dose to the cancerous tissue compared with the dose received by normal tissue during a radiotherapy treatment. Calculations indicate that this dose enhancement can be significant, even 200% or greater. In this paper, the physical and biological parameters affecting this enhancement are discussed. Gold nanoparticles have shown therapeutic efficacy in animal trials and these results are reviewed. Some 86% long-term (>1 year) cures of EMT-6 mouse mammary subcutaneous tumours was achieved with an intravenous injection of gold nanoparticles before irradiation with 250-kVp photons, whereas only 20% were cured with radiation alone. The clinical potential of this approach is also discussed.

Radiotherapy

Radiotherapy remains a major modality of cancer therapy. Improvements include the use of megavolt (6–25 MV) X-rays to avoid skin damage, tomotherapy and intensity-modulated radiation therapy (IMRT) to better concentrate the dose within the shape of the tumour, and better dose fractionation schedules. Despite these advances, radiotherapy may still fail to eradicate tumours due to tumour cells that are radioresistant (e.g. hypoxic), under-irradiated, or outside the targeted region. A sufficient dose can render any tumour cell harmless, but radiotherapeutic doses are limited by potential radiotoxicity to essential normal tissues in the path of the beam. In general, mitotically active tumour tissues are only slightly more susceptible to radiation than are essential normal tissues in the gastrointestinal mucosae, lungs, brain, bone marrow (haematopoiesis) and lymphoid tissues (immunity). Infiltrative cancers, especially those in the nervous system, the neck and the intestines, are particularly difficult to treat. A further limitation of radiation is that the damage to cells is cumulative. DNA strand breaks that are not repaired or other cell damage may not kill a normal cell, but additional irradiation will add to the insult, eventually leading to its demise. This means that a tumour-controlling dose (which inevitably incurs some surrounding normal tissue damage) cannot be repeated with subsequent irradiations (e.g. 6 months later upon tumour regrowth) at the same level, thus resulting in a losing battle.

Radiosensitizers

It would be advantageous to enhance radiation effects in tumours by increasing the dose specifically to the tumour cells. An equipment-based solution to better target tumours is at some point limited since a more precise irradiation volume may exclude important undetectable tumour cells outside the volume. A chemical agent that specifically enhances the radiation effects in the tumour could be more selective at a cellular level. A class of tumour radiosensitizing drugs has been found that is useful in this regard, such as nicotinamide plus carbogen (95% oxygen and 5% carbon dioxide), which was found to enhance radiotherapy of experimental tumours (Nishioka et al 1999). Hypoxic cell radiosensitizers have been found, including 1-(1′,3′,4′-trihydroxy-2′-butoxy)methyl-2-nitroimidazole (RP-343), RP-170 and etanidazole, which showed a sensitization enhancement ratio of about 1.4 (Murayama et al 1993). Using the radioresistant SCCVII strain of mouse squamous cell carcinoma, the prodrug 1-(2′-oxopropyl)-5-fluorouracil (OFU001), which is converted to 5-fluorouracil in-vivo, showed a sensitization enhancement ratio of 1.2 (Shibamoto et al 2001).

Nanoprobes, Inc., 95 Horseblock Road, Yaphank, NY 11980-9710, USA

Correspondence:
James Hainfeld, Research Division, Nanoprobes, Inc., 95 Horseblock Road, Yaphank, NY 11980-9710, USA. E-mail: hainfeld@nanoprobes.com

Radioprotectors

Another approach to improving the effectiveness of radiotherapy is to chemically protect normal tissues. Amifostine has been used in clinical trials of head and neck squamous cell carcinoma patients and appears to be beneficial (Bourhis & Rosine 2002), showing a reduction in xerostomia and radio-induced mucositis, thus minimizing radiation effects while apparently not diminishing tumour control. Animal studies showed rapid uptake of the compound in the salivary glands and subsequent radioprotection. Amifostine has also been found to restore transcriptional activity of p53 (Maurici et al 2001). Its radioprotective factor ranges from 1.1 to 1.3 (Milas et al 1984). More recently, the stable nitroxide Tempol has been shown to convey radioprotection of the salivary glands in C3H mice (Vitolo et al 2004).

Metal Enhanced Radiation Therapy

The strategy underlying our research is to load tumours with gold, which absorbs more X-rays, thus depositing more of the beam's energy there and resulting in a local dose increase specifically to tumour cells (Hainfeld et al 2004).

High-Z dose enhancement therapy

It has long been realized that the dose was increased when a high-Z material was in the targeted zone (Spiers 1949). As far as we know, the earliest biological report appeared more than 30 years ago when chromosomal damage was noticed in circulating lymphocytes from patients undergoing iodine contrast angiography (Adams et al 1977). Other early reports were a study of the cytogenetic effects of contrast media (Norman et al 1978), and measurements in patients of the increased dose during iodine contrast angiography (Callisen et al 1979). In an in-vitro experiment more than 25 years ago, iodine contrast medium was found to radiosensitize cells (Matsudaira et al 1980). To make use of the Auger electrons and the photoelectric effect, iododeoxyuridine (IUdR) was incorporated into cellular DNA in-vitro, yielding a radiotherapeutic advantage of ~3 (Nath et al 1990), as suggested earlier (Fairchild et al 1982). However, this required >20% of the cellular thymine be substituted with IUdR, which would be difficult to achieve in-vivo specifically in a tumour. Theoretical and experimental studies of high-Z dose enhancement over both the megavolt and orthovoltage range have been reported (Das & Kahn 1989; Das & Chopra 1995). Regulla et al (1998, 2002) grew cells on a gold foil that was irradiated (40–120 kVp) and measured a dose enhancement factor (DEF) of more than 100, with secondary electrons travelling over a range of up to 10 μm. Herold et al (2000) injected 1.5–3.0 μm gold particles directly into a tumour followed by irradiation. Excised cells had reduced plating efficiency, but histological examination showed gold particles only at injection sites. Such large particles did not diffuse, hindering tumour coverage. In another study, carried out at the European Synchrotron Radiation Facility, 50-keV monochromatic X-ray beams were used to stereotactically irradiate rat F98 brain gliomas. Prior to the irradiation, the tumours were loaded with 1% iodine by intracarotid injection with mannitol. The measured tumour concentration was 1.0% iodine, with surrounding tissue 0.3%. At ≤15 Gy, life-spans were increased 169%, but at 25 Gy no additional benefit was seen over controls without iodine, presumably due to the excessive damage to normal tissue (i.e. fatality from high doses to normal brain; Adam et al 2006). Santos Mello et al (1983) directly injected tumours with iodine contrast media followed by 100-kVp X-rays and obtained remission in 80% of radioresistant tumours in mice. Norman et al (1997) modified a computed tomography (CT) scanner by inserting a collimator to narrow the beam in both directions to encompass the tumour only (and not the entire subject). This was used to deliver 'tomotherapy-type' conformal orthovoltage (140 kVp) X-rays to spontaneous canine brain tumours after direct tumour injection with iodine contrast media, and 53% longer survival was found. This modified CT was then used in a Phase I human trial of brain tumours using intravenous injection of iodine contrast media (Rose et al 1999). This trial proved the method to be safe and potentially beneficial, although further work is required to establish statistically significant efficacy.

Physics of metal-enhanced radiotherapy

When X-rays impinge on matter, a number of processes can result (Figure 1). The emissions relevant to our discussion are scattered photons (X-rays), photoelectrons, Compton electrons, Auger electrons and fluorescence photons. Radiochemical (free radical and ionization) damage is thereby imparted to the tissue.

When an incident photon ejects an electron from an inner shell of an atom, this photoelectron acquires a kinetic energy of the primary beam minus its binding energy, and this kinetic energy determines the range it will have in the tissue, which can be for example 100 μm or about 10 cell diameters for an electron of about 100 keV energy. This photoelectric effect varies approximately as $(Z/E)^3$, where E is the incident photon energy and Z is the atomic number of the target. For high-Z elements it dominates the interaction with matter at energies <0.5 MeV. The relative effect of gold (Z = 79) to soft tissue (Z = 7.4) in the energy range above gold's K-edge (80.75 keV) is then approximately 1217 (i.e. $79^3/7.4^3$); the ratio is more complicated at lower energies, but still a large number. The photoelectric effect, and in some cases also the inelastic (Compton) scattering, produces atoms in excited states due to the ejected electron. The missing electrons are then restored by electrons falling from higher orbits, which

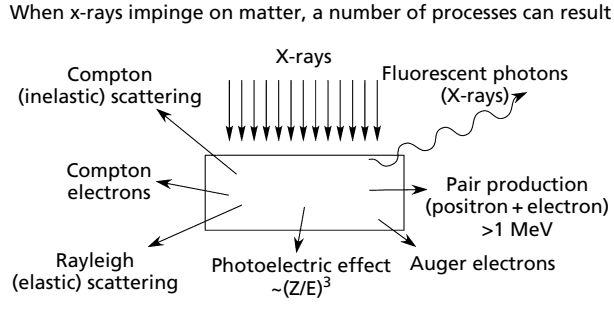

Figure 1 Interaction of X-rays with matter.

release energy either as fluorescent photons or Auger electrons. Fluorescent photons can travel longer ranges (up to centimetres), so, depending on the tumour size, they may or may not provide the desired localized tumour effect. On the other hand, Auger electrons, which are weakly bound electrons ejected as a result of electronic shell rearrangements, can be effective in producing very high local ionization density. However, they travel much shorter distances, typically ~10 nm, and several of them can be emitted from the same atom practically simultaneously. To take advantage of the Auger effect, the emitting atom must be only atoms away from the target molecule to be damaged, for example high-Z atoms intercalated in DNA to cause double-strand breaks. The Auger effect is greater in atoms of medium and high Z.

In Rayleigh (elastic) scattering, photons collide with the entire atom and not with a single electron, and therefore the amount of energy and momentum transferred is negligible. Its cross-section is approximately proportional to Z^2. Rayleigh scattering is most prominent for low-energy photons scattered in high-Z materials. It is peaked in the forward direction. Its cross-section is very small in tissues at energies above 60 keV and in gold above 200 keV. Since this scattering is elastic, virtually no energy is deposited in the tissue and it is not useful for therapy.

Pair production occurs at high photon energies (>1 MeV), where the incident photon energy exceeds twice the rest mass of the electron ($2 \times 0.511 = 1.022$ MeV), resulting in the creation of electron–positron pairs (each having an energy of 0.511 MeV). This effect varies as Z^2, so the relative effect of gold to water is approximately 114 ($79^2/7.4^2$). However, its cross-section in tissue below 3 MeV is completely negligible, and even above that is very small. For gold, photons produced with electron linacs >10 MV may make some difference, but the photoelectric advantage of gold at those beam energies is lost.

Choice of optimal energy

The choice of optimal beam energy for use with a dose-enhancing contrast agent is an important consideration. Since a large effect is predicted over the orthovoltage range (<500 keV) to utilize the relatively large photoelectric cross-section in the high-Z element, this range was chosen for most work. Early radiotherapy was conducted over this range, but the highest dose was upon entry and decreased with depth, thus potentially causing skin damage. It was then realized that megavoltage X-rays would pass through the skin with little interaction, before a build up of the density of the therapeutic, mostly Compton, electrons at depth, thus sparing the skin. Except for treating superficial cancers, most radiotherapy machines now use 6–25-MV electron linacs for the production of X-rays. However, the use of tomotherapy and IMRT, which distribute the entrance dose over a larger area of the patient's skin, could reduce the entrance dose effects if orthovoltages were employed. Rose et al (1999) calculated by Monte Carlo simulations that the local tumour dose could be significantly better than 10 MV irradiation for a deep human brain tumour using 140-kVp photons, delivered tomographically in both cases, if the tumour loading was >0.5% iodine.

What is the best energy for producing the most effective photoelectron yield and dose in the tumour? The attenuation of gold and soft tissue is shown in Figure 2. These attenuation curves show that gold is significantly more absorbent, especially around certain energies. Dividing the two graphs indicates a broad range of superior absorption for gold (Figure 3) by a factor as high as 95 at 20 keV, and 49 just above the K-edge (80.7 keV).

Relative to soft tissue, the best differential contrast from gold is therefore around 20 keV, although other choices also give large factors. However, this beam energy is too low for external-beam radiation therapy of deep tumours due to tissue attenuation. Neglecting that consideration, for maximizing gold absorption, the low energies are best, but other good

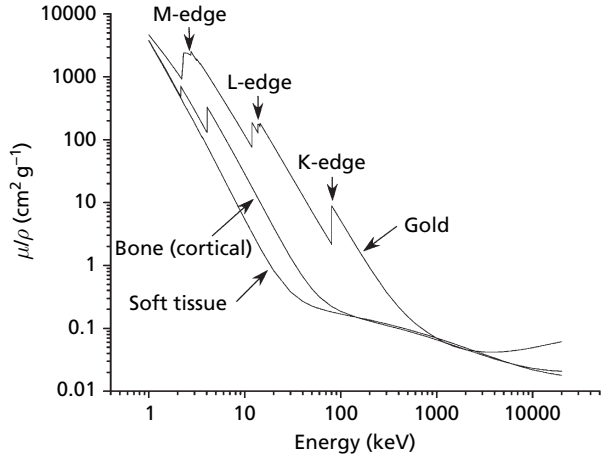

Figure 2 Plot of gold, soft tissue, and bone attenuation versus X-ray energy. For gold, absorption edges occur at: K (80.7 keV), L (L1 14.4 keV; L2 13.7 keV; L3 11.9 keV), and M (2.2–3.4 keV); the K-edge is the energy where the incident energy is just enough to eject an electron from the inner K shell.

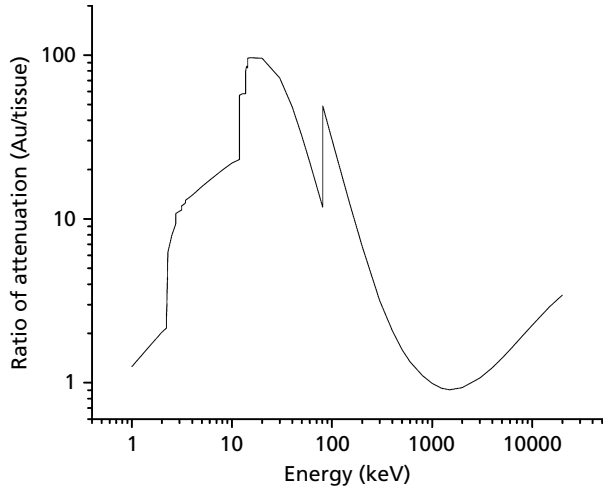

Figure 3 Ratio of gold attenuation compared with soft tissue for the same thickness (gcm^{-2}) of the two materials. A factor of ~100 is obtained at ~20 keV.

choices are just above the K-edge (80.7 keV) and L-edge (L1 14.4, L2 13.7, L3 11.9) energies, where the jump ratios (just above edge to before edge) are 4.2 (for K) and 2.5 (for L3). Although beam energy just above an atomic absorption edge might be best for imaging, it may not be best for therapy. For example, an incident 80.7-keV photon will have all of its energy used in knocking out the K-shell electron, with no kinetic given to the emitted electron. Although some of the 80.7 keV 'invested' in the atom will be deposited locally, the option of using the ejected photoelectric as another vehicle to impart dose to the tissue would not be utilized. That vehicle is particularly important for spreading out the absorbed dose to a group of cells surrounding the point of absorption, thus homogenizing the dose in the target, which can be done mostly by the range of the ejected electron in the tissue. The range of an electron in water (in μm) is approximately $0.1 \times E\ (keV)^{1.5}$, as plotted in Figure 4.

Since cells are 5–10 μm in size, it would seem that a range of several cells might be desirable, that is, use of a beam energy that is 35 keV above an edge for a range of 21 μm. If using energies above the K-edge, one must remember some photoelectric events still occur with the L and M photoelectrons, producing longer range electrons. However, the cross-section for creating photoelectrons drops off with increasing energy above the absorption edge (Figure 2), so some optimal balance is needed. For a range of 40 μm, ~55 keV above the edge is needed, and for gold at 55 keV above the K-edge (135 keV), the absorption is down by a factor of 3.7 from the edge. For the L-edge (11.9 keV), at 55 keV above it (67 keV), the absorption is down by a factor of 57. Typical bremsstrahlung sources have a broad energy spectrum, thus producing a variety of ranging photoelectrons. This is an interesting feature of photon activated therapy, since bystander cells that do not have the high-Z atoms on or in them can be killed. This is in contrast to Boron neutron capture therapy, where the disintegration products of a lithium ion and alpha particle travel only 5 and 9 μm, respectively. Ideally, enough boron must be delivered to each cell in a tumour (although a lesser bystander effect is observed; Kinashi et al 2007), whereas with photon activated therapy, this requirement is relaxed and not all cells need to be loaded to some threshold level. Biologically, tumours are heterogeneous, and targeting schemes based on receptors or antibodies, or almost anything result in heterogeneous distribution of the high-Z material. The effect of electron range in the tumour is a significant advantage for metal-enhanced radiation therapy. What appears to be a practical demonstration of this effect are the results reported by Corde et al (2004), who used a monochromatic X-ray beam at the European Radiation Synchrotron Facility to irradiate cells exposed to iodine compounds. They found the maximal cell kill was not just above the K-edge (edge at 33.169 keV, irradiated at 33.5 keV), but 4.2-times higher cell kill was obtained 17 keV above the K-edge, and 2.1-times higher kill at 37 keV above the K-edge. Enhanced cell killing with IUdR was also found by Karnas et al (1999) to occur with tungsten-filtered 100-kVp X-rays compared with unfiltered 100-kVp X-rays.

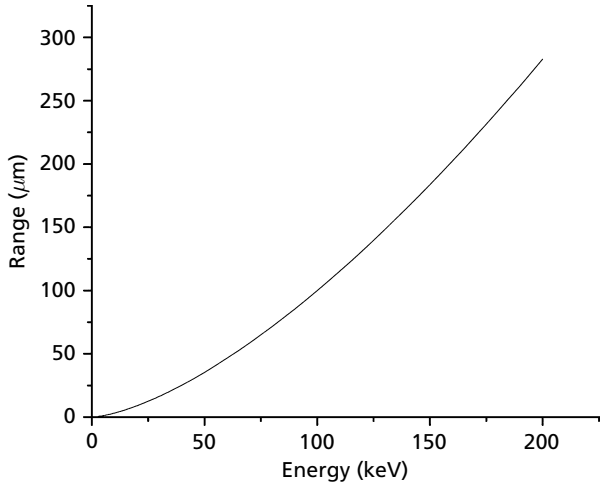

Figure 4 Approximate range of electrons in water versus their energy.

An additional factor for selecting the optimal irradiation energy is the penetration of X-rays to be effective for deep tumours, e.g. of pancreas, liver and brain. Higher energies can deliver more of the dose at depth, since their attenuation in tissue is less (Figure 1). In this regard, gold appears to be preferable over iodine due to its greater absorption at higher energies (2.7-times greater than iodine at 100 keV; Figures 5A and 6A). Some of the attenuated beam is scattered or emitted outside of a typical tumour size or local region, and would not therefore be of value in increasing the tumour dose. For local dose deposition, the energy deposited in a local region should be used, μ_{en}/ρ not μ/ρ. These values are shown in Figures 5B and 6B, and indicate that iodine has an advantage of ~1.9 at 1–2 keV, ~1.4 at 6–10 keV, and 1.4 at 80 keV, whereas gold has an advantage of 3.2 at 4 keV, 3.1 at 30 keV, and ~2.5 at 200–300 keV.

Theoretical calculations of dose enhancement

Some of the intuitive and approximate arguments stated above can be more accurately predicted by Monte Carlo calculations. Several recent theoretical publications have examined various scenarios of loading tumours with high-Z materials and calculated more exact dose enhancements. Robar et al (2002) found that realistic concentrations of iodine or gadolinium contrast media only led to <5% enhancement for "flattened" 6–24-MV photon beams (i.e. filtered to preferentially attenuate the higher spectral yield at lower beam energies), but removal of the flattening filter (allowing photons at lower energies to pass) gave DEFs of 8.4%, 10.8%, 13.7% and 23.1% for 18-MV, 6-MV, 4-MV and 2-MV beams, respectively, with 3% gadolinium in the target tissue. Calculations were for deep brain tumours, and confirmed by measurements of dose in phantoms. Gadolinium contrast media are commonly used to detect brain tumours due to hypervascularity and breakdown of the blood–brain barrier in tumours, which allows the gadolinium agent to selectively penetrate them.

In a similar study, Cho (2005) used Monte Carlo calculations to determine that 3% gold in the tissue would give a 53% enhancement for 2-MV beams without the flattening filter. However, a much larger effect, 560% dose enhancement, could be obtained using a 140-kVp source. For a lower

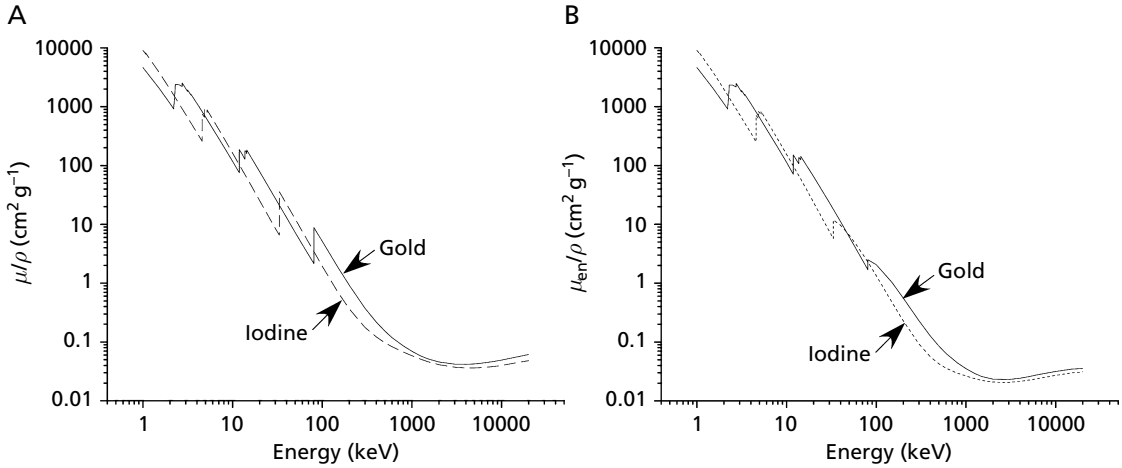

Figure 5 A. Attenuation (μ/ρ) of gold and iodine versus X-ray energy. Each element shows advantages at their electron binding energies. B. Local energy absorption coefficients (μ_{en}/ρ) of gold and iodine versus X-ray energy.

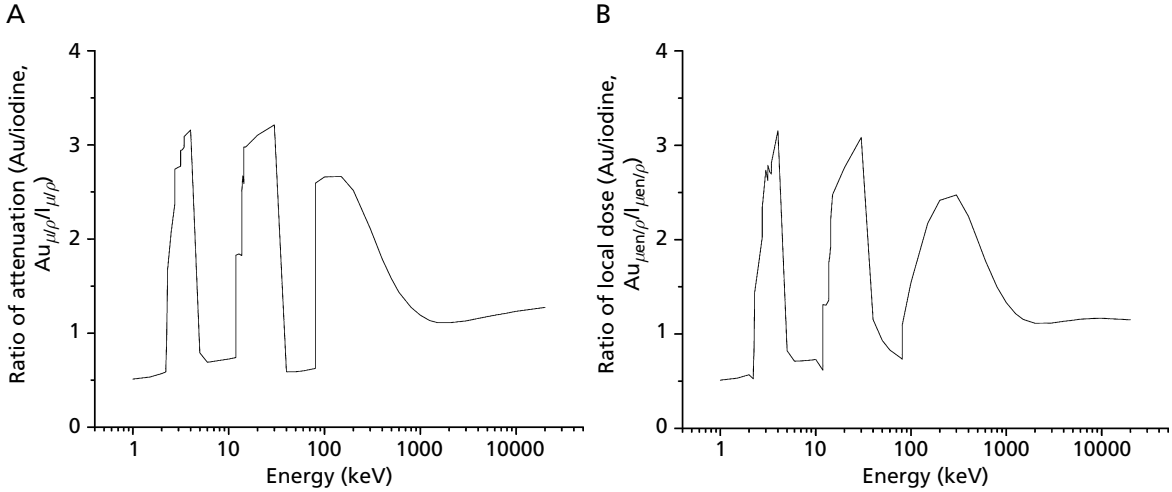

Figure 6 A. Ratio of X-ray attenuation of gold to iodine versus energy. Gold has ~3-fold advantage at ~2, 13–30 and 80–120 keV. B. Ratio of local dose deposition (Au/iodine, $Au_{\mu en/\rho}/I_{\mu en/\rho}$) versus X-ray energy. Gold has a 2.5–3-fold advantage at some energies, whereas iodine is better by 1.5–2-fold at other energies.

loading of gold (0.7%) a 211% dose enhancement was calculated.

Considering the use of a monochromatic synchrotron beam, Boudou et al (2005) calculated using Monte Carlo code that loading a deep brain tumour with 1% iodine would result in a DEF of 2.7 at 35 keV, and confirmed this with phantom experiments.

Roeske et al (2007) did theoretical calculations to find DEFs for all elements Z = 25–90 when irradiated by the most commonly available radiation sources. Instead of Monte Carlo calculations, they used reported elemental attenuation and integrated the absorption over the energy spectrum of the radiation source. For a tissue loading of 0.5% by weight, they found that little enhancement (DEF < 1.05) was obtained using Co-60, Ir-192, Au-198, Cs-137, 6-, 18- and 25-MV X-rays for all elements Z = 25 to 90. For 0.5% gold, a DEF of ~1.65 was calculated when using 80–140-kVp X-rays. Although the DEF generally increases with Z, they noted a decline for elements over the Z = 40–60 range, which includes iodine but not gold (iodine Z = 53, gold Z = 79). Brachytherapy radioisotopes were also considered as radiation sources whose emissions would then be locally absorbed by elements loaded into the tumour or tissue. A DEF (for 0.5% high-Z loading) was <1.05 for Co-60, Ir-192, Au-198 and Cs-137 for all elements, but Pd-103 and I-125 gave DEFs of 1.60 and 1.67, respectively. Pd-103 has a half-life of 17 days, and I-125 a half-life of 60 days. Since the radiation from brachytherapy sources is delivered over roughly this period, it would require that the high-Z material remain in the targeted tissue during that time.

These theoretical papers generally agree that with a high-Z material such as gold, a tissue loading of 0.5–1% by weight can achieve a DEF of ~2 when using conventional 80–140-kVp X-ray tube sources. Although this energy range is available from the X-ray tubes commonly used for planar and CT

imaging, the dose rates are generally lower than desirable and the enhanced dose to the proximal tissue (compared with megavolt therapy) could also be a problem. A more optimal irradiation machine would have a higher power orthovoltage source with IMRT capability, which would enable pre-imaging of the subject to confirm high-Z loading and assist in treatment planning followed by a rotationally applied (tomographic with modulated intensity) therapy dose.

Properties of gold nanoparticles

We reasoned that the use of gold nanoparticles might be of benefit in delivering high-Z material to tumours. Some of the potential advantages of gold nanoparticles include the following.

- Gold absorbs ~3-times more than iodine at 20 and 100 keV.
- The DEF for gold can be 1.2 to >5 depending on the beam's energy and the amount of gold delivered.
- The range of the enhancing effect can be over several cells, for example 100 μm, thus relaxing the requirement that gold be delivered to all tumour cells. Tumours are known to be heterogeneous.
- Gold is relatively inert and can be biocompatible.
- Nanoparticles clear the blood less rapidly than small molecules, such as iodine contrast media that are considered extravascular and exit the vascular system rapidly. Nanoparticles can stay in the blood for hours if designed to do so, thus enhancing tumour delivery.
- Nanoparticles are known to permeate leaky angiogenic endothelium, thus providing some tumour specificity, the so-called enhanced permeability and retention (EPR) effect.
- Nanoparticles have low osmolality.
- Effective tumour targeting with antibodies, peptides or drugs may be possible with nanoparticles. Target sites on tumour cells are limited and one or a few iodine atoms per antibody does not deliver enough high-Z material; conversely one antibody attached to one 15-nm gold nanoparticle would deliver 70 000 gold atoms.
- Gold nanoparticles can be made over a wide range of sizes (1–1000 nm) and designed for best tumour penetration and delivery.
- Gold nanoparticles have a number of surface ligands, allowing flexible design and multifunctionality by incorporating mixed ligands for optimal properties.
- The biodistribution of gold can be imaged before a therapeutic dose is delivered and used for treatment planning and quantified prediction of dose enhancement.
- Other high-Z metal nanoparticles, besides those made of gold, may be used with similar characteristics.

Potential disadvantages or unknowns of gold nanoparticles include the following.

- The high cost of gold.
- Nanoparticles typically clear the body more slowly than some small molecules, leading to longer-term whole-body retention in some cases.
- More complete toxicity studies are needed to assess human use.
- More complete efficacy studies are needed to assess human use.

Some of the properties of gold nanoparticles are attributable to the size used, since a wide range of sizes (0.4–>5000 nm) can be made. However, since gold metal is inert and not metabolized, many of the properties, such as biocompatibility and pharmacokinetics, are largely determined by the stabilizing organic coating and possible surface functionalization. A gold nanoparticle is illustrated in Figure 7. The gold particle has a solid gold core in the zero oxidation state, similar to bulk gold metal. Different synthetic methods have produced shapes other than spheres, including cubes, triangles, cauliflower-like and rods (Wei & Zamborini 2004; Meyer et al 2005; Rodriguez-Fernandez et al 2005). Surface atoms have close to covalent-strength binding affinity to sulfur or phosphorus atoms, so various ligands can be strongly bonded to the gold particle. This allows various functional groups to be attached (R, R′, R″, R‴), such as PEG, carboxyl or amino groups, thiol derivatized drugs, DNA, lipids, carbohydrates or virtually any organic moiety. Reactive groups can be included that will then covalently attach other molecules, such as antibodies or peptides (M2 in diagram). Another approach is to adsorb molecules directly to the gold surface (M1 in diagram). These molecules (e.g. IgG) may not contain free thiols or phosphorus atoms, but can adsorb onto the gold surface by ionic or hydrophobic interactions at multiple sites. These multipoint attachment sites can lead to a strong overall binding, in some cases virtually irreversible. One thing we see is that there is a rich depth of chemistry that can be applied, and that many features can be achieved using this platform. The particles are similar to dendrimers in that they provide numerous functional groups, also dependent on the size. For example, a 0.8-nm particle has seven ligand sites, a 2-nm particle has ~100, and a 15-nm has approximately 4000. There might be an advantage over dendrimers in that a mixture of different ligands can be bound simultaneously (R, R′, R″, R‴) in a simpler construction process. Also, it has been found that completed particles with a ligand shell can undergo substitution of some or all of their ligands, typically by mixing with excess new ligands and heating. The use of multiple ligands and bound molecules confers multiple properties to the particle. For example, two or three targeting moieties can be used, along with S-PEG to avoid reticuloendothelial system uptake. The overall size will

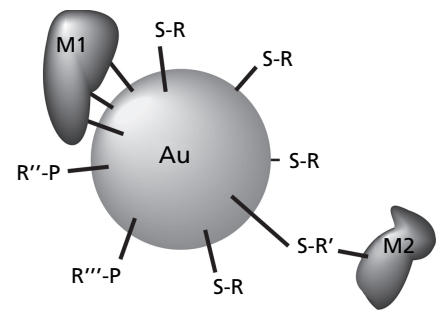

Figure 7 Schematic diagram of gold nanoparticle with ligands. Ligands may be thiols (S-R) or phosphorous (P-R) bound to the surface gold atoms. Mixed ligands may also be used to confer multiple properties (S-R′, P-R′). Molecules (M1 and M2, which can be antibodies, peptides, carbohydrates, nucleic acids, lipids, drugs or other molecules) can be adsorbed to the particle (M1) surface or chemically attached (M2).

also be a strong factor for blood retention time, as well as the surface coating. Small particles can be made that rapidly clear through the kidneys, whereas larger ones avoid kidney filtration. Toxicity may also be controlled by the size and surface coating. Because elemental gold is biologically non-reactive its intrinsic toxicity is low, however all substances are toxic at some level. Optimal design can significantly reduce the toxicity. This discussion is also largely applicable to many other metals and other nanoparticles.

Enhancing tumour radiation dose with high-Z materials is a 'brute force' method, requiring large amounts of the material to be delivered to the tumour. A gold concentration of 0.5% by weight should give a DEF of ~1.6, but better results would be obtained if 1–5% was achieved in the tumour, since tumour cells are formidable adversaries and do not all surrender easily. By weight, 1–5% is huge compared with the doses needed for drugs to kill tumours. For example, in a mouse, ~50 mg taxol kg^{-1} is effective (Milas et al 1995), but for gold enhancement, a dose 50-times that (2500 mg Au kg^{-1}) was needed (Hainfeld et al 2004). Better targeting of the gold would of course reduce the amount needed.

Therapy using gold nanoparticles in mice

For initial trials of enhancing radiation dose with gold nanoparticles, we screened several sizes of gold particles, direct injection in gels, and with and without antibody targeting. More work is needed to fully explore these and other approaches. Our initial approach that was able to achieve >0.5% gold in the tumour for these proof-of-principle studies was intravenous injection of small 1.9-nm gold nanoparticles that were not toxic at the level required (Hainfeld et al 2006). Irradiation was applied shortly after injection (2 min), thus taking advantage of the high gold blood concentration. Tumours are hypervascularized (typically 3–5 times over normal tissue) and irradiation of gold in the blood would result in damage to the endothelium, which is a rational way to treat tumours (anti-angiogenic therapy). Damaging endothelial cells can cut off the blood supply to downstream tumours, resulting in up to 100-times more effectiveness per killed cell compared with killing tumour cells. It also could address a significant problem with radiotherapy, where the central cells, due to rapid tumour growth, squeeze blood vessels and become hypoxic and slow dividing. Radiation has the best effect on rapidly dividing cells, so these hypoxic cells can survive and later cause regrowth of the tumour. By further cutting off the low blood supply to these hypoxic and malnourished cells, they can be killed. These small nanoparticles also leach into tumours through the leaky angiogenic endothelium, thus providing the dose deeper into the tumour tissue.

Biodistribution and pharmacokinetic studies were carried out by intravenously injecting gold nanoparticles into mice with implanted tumours, then dissecting tissues and analysing them for gold content by graphite furnace atomic absorption spectroscopy. A Perkin Elmer 4100Z was used and showed that 5 min post-injection of 1.35 g Au kg^{-1} resulted in 4.9±0.6% injected dose g^{-1} (% ID g^{-1}) in the tumour, with 8.9, 1.4, 2.8, 132 and 18.6% ID g^{-1} in the tumour periphery (which appeared dark at necropsy due to the brown gold particle colour), muscle, liver, kidney and blood respectively. The tumour periphery contained 0.24% gold by weight, and double this injected dose (2.7 g Au kg^{-1}) in the trial (described below) might therefore reach 0.5% gold by weight, which could lead to effective therapy. Since the gold had no targeting ligand, such as an antibody or peptide, its localization in the tumour compared with, for example muscle, is most likely a result of the leaky angiogenic endothelium, an effect well documented by the use of fluorescent dextrans of different sizes (Dvorak et al 1988) and termed the enhanced permeability and retention (EPR) effect (Maeda et al 2000). The blood contained 18.6% ID g^{-1} gold at 5 min. For a dose of 2.7 g Au kg^{-1} in a 20-g mouse with a blood volume of 1.5 mL, the initial blood concentration would be 3.6% Au by weight, and after 5 min, this would drop to 1.0%. Irradiation of this amount of gold in the blood should produce significant dose enhancement to the vasculature, greater than a factor of 2 (according to the above theoretical studies), which could significantly damage the tumour blood supply.

By escalating the dose in mice, it was found that these 1.9-nm gold nanoparticles (commercially available as AuroVist from Nanoprobes, Inc.) had a LD50 of ~3.2 g Au kg^{-1} when administered in phosphate-buffered saline pH 7.4 via tail-vein injection of 0.2 mL. EMT-6 mouse mammary tumours were grown subcutaneously in the upper thigh of Balb/C mice by injecting 10^6 cells. Tumours were grown until they reached a volume of 50–90 mm^3. A short-term (1 month) trial was carried out by irradiating the mice after an injection of 1.35 g Au kg^{-1}. Approximately 2 min after injection, a 2.5-cm diameter region of the leg containing the tumour was irradiated with 250 kVp X-rays through a Thoreaus-1 filter at 5 Gy min^{-1} (30 Gy total) using a clinical Siemens Stabilipan X-ray generator. Tumour volumes were measured along with control animals receiving either no irradiation, irradiation only, or gold without irradiation. The results are shown in Figure 8. Gold without irradiation did not inhibit tumour growth at all, and radiation only slowed tumour growth. With gold prior to irradiation, however, most tumours were undetectable at 1 month. However, many therapies look very promising at 1 month when the tumours shrink considerably, but some tumour cells are

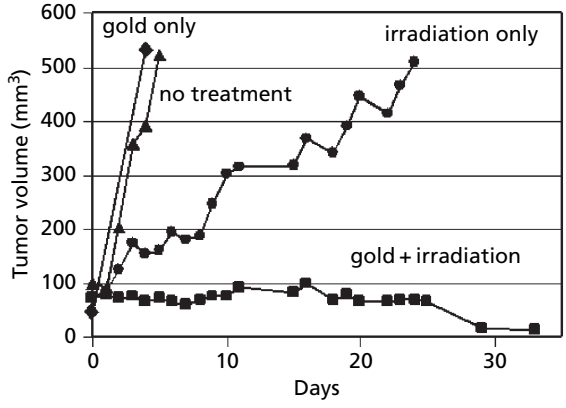

Figure 8 Average tumour volume after: no treatment (▲, n = 12); gold only (♦, n = 4); irradiation only (30 Gy, 250 kVp, ●, n = 11); intravenous gold injection (1.35 g Au kg^{-1}) followed by irradiation (■, n = 10). Reproduced with permission from Hainfeld et al (2004).

not eradicated and the tumours subsequently regrow. We therefore extended the study to more than 1 year and used two levels of gold to determine if a dose response with the amount of gold was evident. The results (Figure 9) showed that there appeared to be a gold dose response. In fact, the gold plus radiation effect was dramatic, resulting in 86% long-term (>1 year) cures at the highest gold dose compared with 20% survival with radiation alone.

The 2.7 g Au kg^{-1}, which gave the best result, is close to the LD50 (~3.2 g Au kg^{-1}). The target organ of toxicity with at least this form and size of gold is the kidney. The lethality has a steep response curve and even though the dose used was close to the LD50, no long-term kidney toxicity was observed at this dose.

Potential of high-Z dose nanoparticle enhancement for clinical therapy

What is the future of metal enhanced radiation therapy? Although a proof-of-principle has been demonstrated with gold nanoparticles, many aspects of the subject need further research. Mouse tumour models are typically 'easy' to treat compared with human pathology, and results in mice are typically more difficult to reproduce in humans. The amount of gold injected for the best results in the study reported here was close to the LD50, so more biocompatible gold (or other high-Z) nanoparticles should be found. Tumour targeting, by placing on the nanoparticles antibodies, peptides, drugs, growth factors or other ligands that are known to bind to tumour cells or tumour vasculature, may improve selective delivery and minimize damage to surrounding normal tissue. The dose enhancement effect is proportional to the amount of high-Z material and receptor-mediated endocytosis might be used to internally load cells. Nuclear localization signal peptides might be able to direct the particles to the nucleus where the Auger emission would be effective. Direct tumour injection has the advantage of delivering the high concentrations required, but may be difficult to implement in real cases due to its invasiveness and the number of injections needed to achieve uniform coverage. Orthovoltage (<500 keV) sources are common for imaging, but would need to have their power increased and perhaps other modifications to be optimal for metal-enhanced radiation therapy. Interestingly, high power X-ray generators in this range have been recently developed for airport baggage screening, and could be adapted for therapeutic use. Use of beam filtration or monochromatic sources could reduce normal tissue absorption and patient dose, and aid in confining the effects to the high-Z material regions. Tomographic application of the radiation with adjustment of the beam geometry and intensity (IMRT) can shape the radiation dose to avoid excessive normal tissue dose or irradiation of important nerves, salivary glands or other tissues that need to be spared. Recently, additional gold nanoparticle radiation enhancement work was reported: gold nanoparticles were mixed with plasmid DNA and found to increase strand breaks by a factor of 2.5 upon irradiation with 60 keV electrons (Zheng et al 2008).

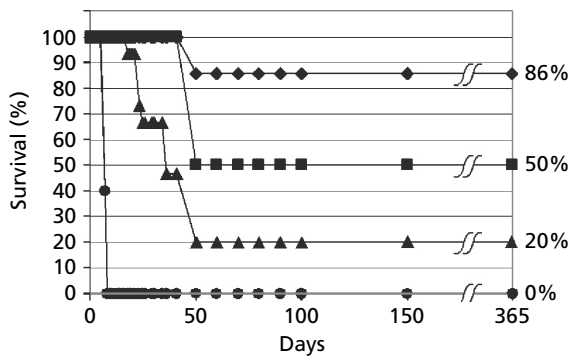

Figure 9 Survival of mice after various treatments of subcutaneous EMT-6 tumours. A gold dose response was evident. ●, No treatment (n = 17), and gold only (1.35 g Au kg^{-1}, no irradiation), indistinguishable from no treatment (n = 4); ▲, irradiation only (26 Gy, 250 kVp), producing 20% long-term (>1 year) survival (n = 15); ■, irradiation after intravenous injection of 1.35 g Au kg^{-1} gold nanoparticles, 50% long-term survival (n = 4); ♦, irradiation after 2.7 g Au kg^{-1} injection, producing 86% long-term survival (n = 7). Reproduced with permission from Hainfeld et al (2004).

Conclusion

Radiotherapy dose enhancement with gold nanoparticles appears to be a promising approach for improved cancer treatment. Nanoparticles, particularly gold nanoparticles, provide a flexible chemical platform for incorporation of various targeting schemes and endowment of desirable properties. Combined with advances in X-ray therapy instrumentation and techniques, specific tumour dose enhancement by gold nanoparticles could significantly improve radiotherapy outcomes.

References

Adam, J. F., Joubert, A., Biston, M. C., Charvet, A. M., Peoc'h, M., Le Bas, J. F., Balosso, J., Esteve, F., Elleaume, H. (2006) Prolonged survival of Fischer rats bearing F98 glioma after iodine-enhanced synchrotron stereotactic radiotherapy. *Int. J. Radiat. Oncol. Biol. Phys.* **64**: 603–611

Adams, F. H., Norman, A., Mello, R. S., Bass, D. (1977) Effect of radiation and contrast media on chromosomes. Preliminary report. *Radiology* **124**: 823–826

Boudou, C., Balosso, J., Esteve, F., Elleaume, H. (2005) Monte Carlo dosimetry for synchrotron stereotactic radiotherapy of brain tumours. *Phys. Med. Biol.* **50**: 4841–4851

Bourhis, J., Rosine, D. (2002) Radioprotective effect of amifostine in patients with head and neck squamous cell carcinoma. *Semin. Oncol.* **29**: 61–62

Callisen, H. H., Norman, A., Adams, F. H. (1979) Absorbed dose in the presence of contrast agents during pediatric cardiac catheterization. *Med. Phys.* **6**: 504–509

Cho, S. H. (2005) Estimation of tumour dose enhancement due to gold nanoparticles during typical radiation treatments: a preliminary Monte Carlo study. *Phys. Med. Biol.* **50**: N163–N173

Corde, S., Joubert, A., Adam, J. F., Charvet, A. M., Le Bas, J. F., Estève, F., Elleaume, H., Balosso, J. (2004) Synchrotron radiation-based experimental determination of the optimal energy for cell radiotoxicity enhancement following photoelectric effect on stable iodinated compounds. *Br. J. Cancer* **91**: 544–551

Das, I. J., Chopra, K. L. (1995) Backscatter dose perturbation in kilovoltage photon beams at high atomic number interfaces. *Med. Phys*. **22**: 767–773

Das, I. J., Kahn, F. M. (1989) Backscatter dose perturbation at high atomic number interfaces in megavoltage photon beams. *Med. Phys*. **16**: 367–375

Dvorak, H. F., Nagy, J. A., Dvorak, J. T., Dvorak, A. M. (1988) Identification and characterization of the blood vessels of solid tumors that are leaky to circulating macromolecules. *Am J. Pathol*. **133**: 95–109

Fairchild, R. G., Brill, A. B., Ettinger, K. V. (1982) Radiation enhancement with iodinated deoxyuridine. *Invest. Radiol*. **17**: 407–416

Hainfeld, J. F., Slatkin, D. N., Smilowitz, H. M. (2004) The use of gold nanoparticles to enhance radiotherapy in mice. *Phys. Med. Biol*. **49**: N309–N315

Hainfeld, J. F., Slatkin, D. N., Focella, T. M., Smilowitz, H. M. (2006) Gold nanoparticles: a new X-ray contrast agent. *Br. J. Radiol*. **79**: 248–253

Herold, D. M., Das, I. J., Stobbe, C. C., Iyer, R. V., Chapman, J. D. (2000) Gold microspheres: a selective technique for producing biologically effective dose enhancement. *Int. J. Radiat. Biol*. **76**: 1357–1364

Karnas, S. J., Yu, E., McGarry, R. C., Battista, J. J. (1999) Optimal photon energies for IUdR K-edge radiosensitization with filtered X-ray and radioisotope sources. *Phys. Med. Biol*. **44**: 2537–2549

Kinashi, Y., Masunaga, S., Nagata, K., Suzuki, M., Takahashi, S., Ono, K. (2007) A bystander effect observed in boron neutron capture therapy: a study of the induction of mutations in the HPRT locus. *Int. J. Radiat. Oncol. Biol. Phys*. **68**: 508–514

Maeda, H., Wu, J., Sawa, T., Matsumura, Y., Hori, K. (2000) Tumor vascular permeability and the EPR effect in macromolecular therapeutics: a review. *J. Control. Release* **65**: 271–284

Matsudaira, H., Ueno, A. M., Furuno, I. (1980) Iodine contrast medium sensitizes cultured mammalian cells to X-rays but not to gamma rays. *Radiat. Res*. **84**: 144–148

Maurici, D., Monti, P., Campomenosi, P., North, S., Frebourg, T., Fronza, G., Hainaut, P. (2001) Amifostine (WR2721) restores transcriptional activity of specific p53 mutant proteins in a yeast functional assay. *Oncogene* **20**: 3533–3540

Meyer, D. A., Oliver, J. A., Albrecht, R. M. (2005) A method for the quadruple labeling of platelet surface epitopes for transmission electron microscopy. *Microsc. Microanal*. **11**: 142–143

Milas, L., Hunter, N., Ito, H., Peters, L. J. (1984) Effect of tumor type, size, and endpoint on tumor radioprotection by WR-2721. *Int. J. Radiat. Oncol. Biol. Phys*. **10**: 41–48

Milas, L., Hunter, N. R., Kurdoglu, B., Mason, K. A., Meyn, R. E., Stephens, L. C., Peters, L. J. (1995) Kinetics of mitotic arrest and apoptosis in murine mammary and ovarian tumors treated with taxol. *Cancer Chemother. Pharmacol*. **35**: 297–303

Murayama, C., Suzuki, A., Sato, C., Tanabe, Y., Shoji, T., Miyata, Y., Nishio, A., Suzuki, T., Sakaguchi, M., Mori, T. (1993) Radiosensitization by a new potent nucleoside analog: 1-(1′,3′,4′-trihydroxy-2′-butoxy)methyl-2-nitroimidazole(RP-343). *Int. J. Radiat. Oncol. Biol. Phys*. **26**: 433–443

Nath, R., Bongiorni, P., Rockwell, S. (1990) Iododeoxyuridine radiosensitization by low- and high-energy photons for brachytherapy dose rates *Radiat. Res*. **124**: 249–258

Nishioka, A., Ohizumi, Y., Lam, G. K., Pickles, T. A., Chaplin, D. J., Ogawa, Y., Inomata, T., Yoshida, S. (1999) The effects of nicotinamide plus carbogen or pions for microscopic SCCVII tumors. *Oncol. Rep*. **6**: 583–586

Norman, A., Adams, F. H., Riley, R. F. (1978) Cytogenetic effects of contrast media and triiodobenzoic acid derivatives in human lymphocytes. *Radiology* **129**: 199–203

Norman, A., Ingram, M., Skillen, R. G., Freshwater, D. B., Iwamoto, K. S., Solberg, T. (1997) X-ray phototherapy for canine brain masses *Radiat. Oncol. Investig*. **5**: 8–14

Regulla, D. F., Hieber, L. B., Seidenbusch, M. (1998) Physical and biological interface dose effects in tissue due to X-ray-induced release of secondary radiation from metallic gold surfaces *Radiat. Res*. **150**: 92–100

Regulla, D., Schmid, E., Friedland, W., Panzer, W., Heinzmann, U., Harder, D. (2002) Enhanced values of the RBE and H ratio for cytogenetic effects induced by secondary electrons from an X-irradiated gold surface. *Radiat. Res*. **158**: 505–515

Robar, J. L., Riccio, S. A., Martin, M. A. (2002) Tumour dose enhancement using modified megavoltage photon beams and contrast media. *Phys. Med. Biol*. **47**: 2433–2449

Rodriguez-Fernandez, J., Perez-Juste, J., Mulvaney, P., Liz-Marzan, L. M. (2005) Spatially-directed oxidation of gold nanoparticles by Au(III)-CTAB complexes. *J. Phys. Chem. B*. **109**: 14 257–14 261

Roeske, J. C., Nunez, L., Hoggarth, M., Labay, E., Weichselbaum, R. R. (2007) Characterization of the theoretical radiation dose enhancement from nanoparticles. *Technol. Cancer Res. Treat*. **6**: 395–402

Rose, J. H., Norman, A., Ingram, M., Aoki, C., Solberg, T., Mesa, A. (1999) First radiotherapy of human metastatic brain tumors delivered by a computerized tomography scanner (CTRx). *Int. J. Radiat. Oncol. Biol. Phys*. **45**: 1127–1132

Santos Mello, R., Callisen, H., Winter, J., Kagan, A. R., Norman, A. (1983) Radiation dose enhancement in tumors with iodine. *Med. Phys*. **10**: 75–78

Shibamoto, Y., Zhou, L., Hatta, H., Mori, M., Nishimoto, S. I. (2001) In vivo evaluation of a novel antitumor prodrug, 1-(2′-oxopropyl)-5-fluorouracil (OFU001), which releases 5-fluorouracil upon hypoxic irradiation. *Int. J. Radiat. Oncol. Biol. Phys*. **49**: 407–413

Spiers, F. W. (1949) The influence of energy absorption and electron range on dosage in irradiated bone. *Br. J. Radiol*. **22**: 521–533

Vitolo, J. M., Cotrim, A. P., Sowers, A. L., Russo, A., Wellner, R. B., Pillemer, S. R., Mitchell, J. B., Baum, B. J. (2004) The stable nitroxide tempol facilitates salivary gland protection during head and neck irradiation in a mouse model. *Clin. Cancer Res*. **10**: 1807–1812

Wei, Z., Zamborini, F. P. (2004) Directly monitoring the growth of gold nanoparticle seeds into gold nanorods. *Langmuir* **20**: 11 301–11 304

Zheng, Y., Hunting, D. J., Ayotte, P., Sanche, L. (2008) Radiosensitization of DNA by gold nanoparticles irradiated with high-energy electrons. *Radiat. Res*. **169**: 19–27